

**KERNFORSCHUNGSZENTRUM  
KARLSRUHE**

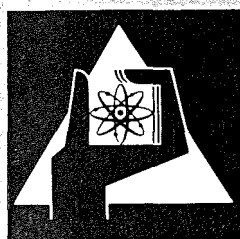
June 1972

KFK 1676

Institut für Angewandte Kernphysik  
Projekt Schneller Brüter

**Progress on Neutron Cross Section Measurements  
at Karlsruhe**

S. Cierjacks



**GESELLSCHAFT  
FÜR  
KERNFORSCHUNG M.B.H.**

**KARLSRUHE**

Als Manuskript vervielfältigt

Für diesen Bericht behalten wir uns alle Rechte vor

GESELLSCHAFT FÜR KERNFORSCHUNG M. B. H.  
KARLSRUHE

KERNFORSCHUNGSZENTRUM KARLSRUHE

KFK 1676

Institut für Angewandte Kernphysik  
Projekt Schneller Brüter

Progress on Neutron Cross Section Measurements  
at Karlsruhe

S. Cierjacks

Gesellschaft für Kernforschung m.b.H., Karlsruhe

Invited Paper

Annual Meeting of the American Nuclear Society, Las Vegas,  
Nevada, June 18 - 22, 1972



## Abstract:

Recent measurements of technologically important nuclear data at the pulsed 3 MV Van-de-Graaff accelerator and the fast neutron time-of-flight spectrometer at the isochronous cyclotron are described. Mainly three types of experiments have been carried out at the Van-de-Graaff accelerator: Measurements of capture-to-fission cross section ratios, high resolution neutron total and neutron resonance capture cross sections and determinations of fission cross sections. In the last two years the activity at the fast neutron spectrometer has been concentrated on the measurement of  $\gamma$ -ray production cross sections,  $(n,x)$  reaction cross sections, fission cross sections and elastic scattering experiments at a few angles. To enable measurement of absolute partial neutron cross sections two methods have been developed to accurately determine the fast neutron flux using the well known n-p cross section as a standard. The two methods are briefly described. Finally, a short review is given of the neutron data program adopted by Karlsruhe for the next two years.

## Zusammenfassung:

Dieser Bericht gibt einen Überblick über Karlsruher Messungen technologisch wichtiger Kerndaten mit dem 3 MV Van-de-Graaff Beschleuniger und dem großen Flugzeitspektrometer am Isochron Zyklotron. Am Van-de-Graaff Beschleuniger wurden in letzter Zeit vor allem drei Typen von Experimenten durchgeführt: Messungen von Einfang- zu Spaltquerschnittsverhältnissen, Bestimmungen hochaufgelöster Gesamt- und n-Einfangquerschnitte, sowie Messungen von Spaltquerschnitten. Die Kerndatenaktivitäten am Zyklotron haben sich in den letzten zwei Jahren auf die Messung von  $\gamma$ -Produktionsquerschnitten, von  $(n,x)$ -Reaktionsprozessen, von Spaltquerschnitten für schnelle Neutronen und auf Experimente zur elastischen Neutronenstreuung konzentriert. Um Absolutmessungen partieller Neutronenquerschnitte zu ermöglichen, werden zwei Methoden zur Flußbestimmung angewandt. Die beiden Methoden, bei denen der bekannte n-p Streuquerschnitt als Standard dient, werden beschrieben. Der Bericht schließt mit einem Ausblick auf das Karlsruher Kerndatenprogramm für die nächsten zwei Jahre ab.



Progress on Neutron Cross Section Measurements  
at Karlsruhe

S. Cierjacks

Institut für Angewandte Kernphysik  
Kernforschungszentrum Karlsruhe, Karlsruhe  
F.R. Germany

Abstract:

Recent measurements of technologically important nuclear data at the pulsed 3 MV Van-de-Graaff accelerator and the fast neutron time-of-flight spectrometer at the isochronous cyclotron are described. Mainly three types of experiments have been carried out at the Van-de-Graaff accelerator: Measurements of capture-to-fission cross section ratios, high resolution neutron total and neutron resonance capture cross sections and determinations of fission cross sections. In the last two years the activity at the fast neutron spectrometer has been concentrated on the measurement of  $\gamma$ -ray production cross sections,  $(n,x)$  reaction cross sections, fission cross sections and elastic scattering experiments at a few angles. To enable measurement of absolute partial neutron cross sections two methods have been developed to accurately determine the fast neutron flux using the well known n-p cross section as a standard. The two methods are briefly described. Finally, a short review is given of the neutron data program adopted by Karlsruhe for the next two years.

I. Introduction

During the last six years Neutron Cross Section measurements have been carried out at Karlsruhe using two main facilities: The pulsed 3 MV Van-de-Graaff accelerator and the Karlsruhe isochronous cyclotron.





The 3 MV Van-de-Graaff with top terminal pulsing and Mobley buncher is capable of producing 10 mA proton pulses with 1 nsec duration. The  ${}^7\text{Li}(p,n){}^7\text{Be}$  reaction is used for neutron production in the energy range from  $\sim 10$  keV to 1.2 MeV. In neutron cross section measurements the thin target technique is used for production of monoenergetic neutrons as well as the time-of-flight technique with production of continuous neutron spectra from thick targets.

The fast neutron spectrometer installed at the isochronous cyclotron provides  $\sim 1$  nsec pulses with a time average neutron intensity of  $\sim 2 \cdot 10^{13}$  n/sec.sr in the forward direction. Bombardment of a natural uranium target with 45 MeV deuterons from the internal beam yields a continuous neutron spectrum allowing for neutron measurements between a few hundred keV and 30 MeV with flight path lengths of 60 and 195 m.

The nuclear data programs for both facilities have been mainly directed to the cross sections needs of the DeBeNeLux Fast Breeder Project. In particular, measurements of  $\alpha$ , high resolution total, capture and fission cross sections of technologically important materials have been made with the Van-de-Graaff. Measurements at the cyclotron have been devoted to very high resolution total cross sections, the determination of elastic and inelastic scattering data (n,x)-reactions and fission cross sections in the energy range from a few hundred keV to 30 MeV.

Because I cannot possibly summarize all the results which have already been obtained, this talk will be limited to progress in neutron cross section measurements at Karlsruhe since the last Neutron Cross Section Conference in Knoxville. In addition, I shall present final results for certain important cross sections and ratios for which only preliminary values had been given in the past.

## II. Cross Section Measurements at the Van-de-Graaff Accelerator

### A. Capture-to-Fission Cross Section Ratios

Because of their importance for the design of advanced fast breeder reactors a high priority in our nuclear data program is given to the measurement of capture-to-fission ratios,  $\alpha$ . Recently Bandl et al. have completed deter-

mination of  $\alpha$ -values for  $^{235}\text{U}$  and  $^{239}\text{Pu}$  in the energy region from 8 to 60 keV. The measurements were carried out by a new technique based on neutron detection only. The method which is similar to that first adopted by Farley et al. <sup>1)</sup> for the resonance region was modified for use in the keV-region where neutron scattering can no longer be neglected with respect to absorption.

The experimental setup which is shown in fig. 1 consisted of a four detector device: The absorption was measured by a comparison of the scattered (i.e. slow) neutron intensity from the fissile sample with that from a non-absorbing lead sample of the same transmission. A  $^6\text{Li}$ -glass scintillator was used for the scattered neutron detector. An equivalent detector with a neutron insensitive  $^6\text{Li}$ -depleted glass scintillator served for  $\gamma$ -ray background determination. The fast fission neutrons were simultaneously detected with an organic liquid scintillator provided with pulse shape discrimination against  $\gamma$ -background. An additional neutron monitor was used for intercorrelations of runs. The further necessary transmission measurements were performed in a separate run using a  $^6\text{Li}$ -glass detector for low neutron counting. A pulsed beam time-of-flight technique was applied for neutron energy determination.

The final values of the capture-to-fission ratios of Bandl, Mießner and Fröhner are plotted in figs. 2-3 as solid circles. The  $\alpha$  values of  $^{239}\text{Pu}$  are compared with previous results in the top curve, while fission-to-capture ratios for  $^{235}\text{U}$  are shown together with the data from other laboratories in the bottom curve. In obtaining the absolute ratios Bandl et al. normalized their measured shape of  $\alpha$  versus E to an average of the data of de Saussure et al. <sup>2)</sup> and of Hopkins and Diven <sup>3)</sup> for  $^{239}\text{Pu}$  and to the data of Alter and Dunford <sup>4)</sup> for  $^{235}\text{U}$  in the energy range from 40 - 50 keV. The error bars (shown for a few data points) correspond to statistical and systematic uncertainties which range from 14 % at 10 keV to 18 % at 50 keV for Pu and from 15 % to 13 % for U at the corresponding energies. Inspection of the Pu data below 15 keV shows that the Karlsruhe data tend to support the data of Schomberg et al. <sup>5)</sup>. Bandl's shape curves for both U and Pu exhibit a fine structure which is believed to be significant, because the same structure has been reproduced in three independent runs. In addition, similar structure has been observed near 14 keV by Farrel et al. <sup>6)</sup> in the bomb shot measurements. The appearance of intermediate structure due to subthreshold fission might be a possible explanation <sup>7)</sup>.

B. High Resolution Neutron Total and Neutron Resonance Capture Cross Section Measurements.

A long term program of high resolution transmission and capture measurements with separated isotopes in the many keV energy range is being pursued by Beer, Ernst, Spencer and Fröhner. In addition to  $^{57}\text{Fe}$  and  $^{53}\text{Cr}$  (investigated by Rohr and Müller) Beer et al. have recently made transmission measurements for the isotopes  $^{54}\text{Fe}$ ,  $^{50}\text{Cr}$ ,  $^{62}\text{Ni}$ ,  $^{64}\text{Ni}$  and  $^{52}\text{Cr}$ . These measurements were performed with a resolution ranging between 0.2 - 0.6 nsec/m (the flight path length was varied because of the available amount of sample material) which was sufficient to resolve all s-wave levels below 200 keV. fig. 4 illustrates a new total cross section measurement of  $^{50}\text{Cr}$  from 20 - 290 keV by Beer and Spencer. Transmission data for two different sample thicknesses of Cr-oxide ( $o = .03 \text{ Cr at/b}$  and  $x = .05 \text{ Cr at/b}$ ) are shown in the figures. The curves drawn through these data represent a multilevel least-squares fit to both sample thicknesses simultaneously. Energy resolution and Doppler-broadening effects were taken into account. The resonance parameters obtained from the fit to  $^{50}\text{Cr}$  are given along with the parameters for a similar fit to  $^{64}\text{Ni}$  in table 1.

Samples of analysed resonances in the range from 10 to a few hundred keV are statistically large enough to reliably determine s-wave strength functions. Such results then can be used for comparison with optical model calculations modified to take into account shell- and pairing effects which are expected to yield a good description of the rapid strength function fluctuations with mass number <sup>8)</sup>.

The measurements of high resolution radiative capture cross sections of enriched samples of medium weight nuclei started by Kompe and Ernst in 1968 have been continued during the last three years by Beer, Ernst, Spencer and Fröhner. In addition to the results obtained for  $^{47}\text{Ti}$ ,  $^{56}\text{Fe}$ ,  $^{58}\text{Ni}$ ,  $^{60}\text{Ni}$  and  $^{61}\text{Ni}$  new measurements have been performed for  $^{57}\text{Fe}$ ,  $^{54}\text{Fe}$ ,  $^{50}\text{Cr}$  and  $^{53}\text{Cr}$  and preliminary results for these nuclei are available. In the experiments a well-collimated neutron beam is passed through a cylindrical hole in the 1 m diameter liquid scintillator tank. The samples are exposed in the center of the tank at a distance of 2 m from the target. Neutron energies are determined by the time-of-flight technique. The time resolution in standard measurements is 2 ns/m. For determination of absolute capture cross sections the  $^{197}\text{Au}$

(n, $\gamma$ )-cross section was used as a standard.

A preliminary result for the capture cross section of  $^{57}\text{Fe}$  between 10 - 150 keV is shown in fig. 5. It should, however be noted, that this data has not yet been corrected for the effects of resonance self-shielding, multiple scattering and resolution broadening.

Using the resonance spins and neutron widths from the total cross section analysis makes it possible to extract a large number of radiation widths, particularly for most of the broad s-wave resonances. The calculation of radiation widths for  $^{57}\text{Fe}$  and  $^{54}\text{Fe}$  is in progress but has not yet been finished.

A sufficient sample of neutron and radiation widths will allow further to verify the existence of non-statistical effects in resonance capture as predicted theoretically by Lane <sup>9)</sup> and apparently observed in the mass 50 - 60 region by the RPI group <sup>10)</sup>. An investigation of this type is presently being made in Karlsruhe by Beer and Spencer.

### C. Fission Cross Sections

A series of fission experiments have been carried out at Karlsruhe by Käppeler and Pflöschinger over the last few years. In the early stages these activities were concentrated on the measurements of fission cross section ratios. At present results are available for  $\sigma_f^{233}\text{U}/\sigma_f^{235}\text{U}$ ,  $\sigma_f^{239}\text{Pu}/\sigma_f^{235}\text{U}$  and  $\sigma_f^{241}\text{Pu}/\sigma_f^{235}\text{U}$  in the energy range from 10 keV to 1.2 MeV. More recently strong effort has also been made on the determination of absolute fission cross sections using the well known n-p cross section as a standard.

Two types of detectors which have been used in these investigations are shown in fig. 6. Both fission counters are gas scintillation chambers filled with an argon/nitrogen mixture at atmospheric pressure. They are used for counting single fission fragments to investigate samples with low  $\alpha$ -activities (upper detector) and for counting both fragments in coincidence from samples with high  $\alpha$ -activities (lower detector). In ratio measurements two identical chambers of the "lower" type (one containing the  $^{235}\text{U}$  sample, the other the corresponding material in question) were symmetrically arranged

at the same distance from the source and exposed to the same neutron flux. In the absolute cross section measurement a chamber of the "upper" type was used back-to-back with a telescope-like proton recoil detector details of which will be discussed in section IV.

A recently completed determination of the fission cross section ratio of  $\sigma_f^{241\text{Pu}}/\sigma_f^{235\text{U}}$  is shown in fig. 7. These data supersede the preliminary results (the mass determination by CBNM Geel was not available at that time) presented at the Helsinki Conference. The uncertainties of the fission cross section ratios are between 1 and 3 %. In this figure Käppeler's data (full circles) are compared with results from other laboratories. In the region from about 150 - 400 keV the data of Butler <sup>11)</sup> and from 400 - 1200 keV the data of Smith, Smith and Henkel <sup>12)</sup> disagree with the Karlsruhe measurements. This may partially be due to structure effects which do not show up in the results from the other laboratories but which clearly appear in Käppeler's data. Evidence for such structure also comes from recent results of the Harwell group <sup>13)</sup> (not shown in this figure).

New absolute fission cross section results for  $^{235}\text{U}$  measured by Käppeler in the energy range from 0.5 - 1.2 MeV became available shortly before I left Karlsruhe. These results for the  $^{235}\text{U}$  fission cross section determined relative to the n-p cross section are shown in fig. 8. The data have an absolute uncertainty of 3-4 %, but, must be considered preliminary, since mass determinations need final verification. However, the additional mass determination is expected to give less than 2 - 3 % change in the absolute cross section. The two different symbols used for the Karlsruhe data require an explanation: While the data indicated by solid squares were obtained by a back-to-back measurement of the fission chamber and the proton telescope, the solid circles were obtained by placing both detectors at different distances from the target. To avoid additional correction due to geometry effects the latter values were only used to define the cross section shape and then normalized at the corresponding energies for which exact values have been obtained. It can be seen that Käppeler's data support the results of White <sup>14)</sup>, Szabo et al. <sup>15)</sup> and the data of Simirenkin <sup>16)</sup> rather than those of Poenitz <sup>17)</sup>.

### III. Cross Section Measurements at the Cyclotron

#### A. High Resolution $\gamma$ -Ray Production Cross Sections

An accurate knowledge of cross sections for the production of  $\gamma$ -rays from neutron inelastic scattering over a wide energy range is essential for reliable radiation transport calculations. To meet this need a new spectrometer employing a Ge(Li)-detector for  $\gamma$ -ray detection was setup at the cyclotron in 1970 by Voß, Kropp and Cierjacks. The experimental arrangement is shown in fig. 4. The ring scatterer (located at the 60 m station) was viewed at a backward angle of  $125^\circ$  by a  $40\text{ cm}^3$  Ge(Li) detector. The detector (shielded from the direct neutron beam by a suitably shaped collimator) provides a time-signal to determine the incident neutron energy and an analog signal to identify specific  $\gamma$ -transitions in the residual nucleus.

This device was used to determine cross sections for the production of six  $\gamma$ -lines from inelastic scattering in Al and five  $\gamma$ -lines from inelastic scattering in Fe. Final cross sections for the production of the 2209 keV  $\gamma$ -ray in Al are given in Fig. 5 for the energy region from threshold to 13 MeV. Total cross sections for the different  $\gamma$ -transitions have been obtained by multiplying the differential data at  $125^\circ$  by  $4\pi$ . The data which have a statistical uncertainty of 8 % at 4 MeV and 5 % at 13 MeV exhibit significant structure. All excitation functions have been analyzed for determination of average level widths and to search for intermediate structure. Evidence was found for channel correlated structure which might be an indication of doorway states <sup>18)</sup>.

#### B. High Resolution Total and Differential Elastic Resonance Cross Sections

A program of combined transmission and differential elastic cross section measurements has been started by Nebe and Kirouac. The primary purpose of this work was to determine spins and parities of resolved but closely spaced resonances of medium weight nuclei in the MeV-region by a study of resonance shapes and symmetry properties. It has been shown <sup>19)</sup> that the shapes are very sensitive to the  $l$ -value of a resonance state due to the interference between resonance scattering and the hard sphere scattering from other partial waves. Thus, a few properly chosen angles allow a unique determination of the  $l$  and  $J$  values.

Since such investigations require highly resolved data, the scattering sample was placed 60 m from the source. Three proton recoil detectors were employed at  $54^\circ$ ,  $90^\circ$  and  $140^\circ$  to the incident beam direction at a short distance from the sample for simultaneously counting of the scattered neutrons.

Differential elastic scattering cross sections were obtained for  $^{40}\text{Ca}$  between 0.5 - 3.5 MeV and are shown from 0.75 - 1.15 MeV in fig. 11<sup>20)</sup>. A comparison of the measured resonance shapes at the three characteristic angles with those calculated from theory allowed the assignment of  $l$  and  $J$  values for about 70 levels in the investigated energy region from 0.55 - 2.0 MeV. Using the spin and parities assignments from the differential scattering allowed the unambiguous determination of neutron widths from a multilevel least squares shape analysis of the total neutron cross sections for the sufficiently broad s-p- and d-wave resonances. The resonance parameters obtained from the fits to  $^{40}\text{Ca}$  are summarized in table 2. The samples of analyzed resonances were large enough to determine accurate s-,p- and d-wave strength functions<sup>21)</sup>.

### C. (n-x)-Reaction Cross Sections

Due to the increasing requirement of (n,x)-reaction data for the field of radiation damage research and for study of certain technological problems in fusion reactions, the measurement of (n,x)-reaction cross sections, especially (n, $\alpha$ )-reactions, will strongly be intensified in our future program. Cross section for the  $^9\text{B}(n,\alpha)$ -reaction have been measured in the past by Kropp and Forti. To determine excitation functions along with the energy- and angular distributions of the emitted charge particles, a three parameter experiment was performed using solid state telescopes for charge particle detection and identification. A schematic drawing of the scattering chamber used by Kropp et al. is shown in fig. 11. Three telescopes each consisting of a thin ( $60\mu$ ) dE/dx- and a thick ( $500\mu$ )  $E_R$ -silicon detector are positioned 11 cm from the sample at a fixed angle to the sample foil. An additional telescope consisting of three solid state detectors was used for absolute flux measurements for which the n-p cross sections again served as a standard. While particle identification was accomplished with the specific dE/dx information, the incident neutron energy was determined by the time-of-flight determination.

Some typical results obtained with the spectrometer are shown in fig. 13. Here excitation functions of the  $^9\text{Be}(n,\alpha)^6\text{He}$  reaction (data for the ground

state transition were extracted from the measured energy distributions) are plotted for six characteristic scattering angles between  $20^\circ$  and  $140^\circ$ . For the lowest incident neutron energies no differential cross sections could be determined for large emission angles because of the low charged particle energies. The actual moderate energy resolution of incident neutrons and charged particles which have been obtained so far will be improved in future experiments by decreasing sample thicknesses and increasing the flight path length from 4 m to 12 m.

#### D. Fission Cross Section

In addition to the experiments in the many keV region at the Van-de-Graaff accelerator fast neutron fission cross section measurements between 0.5 - 30 MeV have been performed at the cyclotron by Cierjacks, Brotz, Gröschel, Kopsch, Nebe, Newstead, Schmalz and Voß. To date data are available for  $^{235}\text{U}$  and  $^{238}\text{U}$ . In these experiments a newly designed fission-spectrometer (described at the 1971 Knoxville Conference) was used. A combination of nine gas scintillation chambers in series (the chambers are similar to the one shown in the lower part of fig. 6) served as the fission detector. To determine the ratio of  $\sigma_f^{238}\text{U}/\sigma_f^{235}\text{U}$  along with the absolute cross section for the two nuclei separately four fission foils of  $^{235}\text{U}$  and four foils of  $^{238}\text{U}$  were irradiated simultaneously at the 60 m station. For absolute cross section determination the neutron flux was measured by a back to back arrangement of the fission detector and two proton recoil telescopes which will be described in section IV.

First results of the fission cross section ratio  $\sigma_f^{238}\text{U}/\sigma_f^{235}\text{U}$  are shown in fig. 14. Below 2 MeV the open circles indicate an energy average over 50 keV intervals of the original data. From 2 - 9 MeV energy averages over 200 keV were taken. The error bars (shown for a few data points) correspond to statistical uncertainties only. Since accurate mass determination have not yet become available, the measured shape of the fission cross section ratio versus energy was normalized to the recommended value of Hart <sup>22)</sup> at 14 MeV. Except for the prominent peak at 7 MeV which showed up only in the Karlsruhe data and those of Smith et al. <sup>23)</sup> our shape curve is in general agreement with that of White and Warner <sup>24)</sup>.



Together with the results from the flux detectors the fission cross section of  $^{235}\text{U}$  and  $^{238}\text{U}$  will be determined separately relative to the n-p-scattering cross section. This work is in progress.

#### IV. Absolute Neutron Flux Determination

For neutron energies above  $\sim 100$  keV any partial cross section can be determined with high accuracy only if it refers to the hydrogen n,p-scattering cross section. This is the only standard cross section established by experimental and theoretical work by better than 2 % up to energies of 50 MeV.

Therefore, considerable effort was made in the past to design suitable proton detector assemblies for fast neutron flux measurements. The two systems now in use at Karlsruhe for standard absolute partial cross section measurements are shown in fig. 15 in a simplified schematic drawing. The telescope-like proton recoil detector at the left side of this figure was developed in its specific form by Käppeler and Fröhner for flux measurements in the energy region from  $\sim 200$  keV to a few MeV. Protons produced in a thin radiator foil of stearin acid are detected by a silicon solid state detector with a sensitive area of  $\sim 4 \text{ cm}^2$ . The detector geometry is chosen so that only forward-peaked protons are detected. This gives rise to defined experimental conditions, but reduces the detector efficiency. A typical value for this quantity is  $4 - 8 \cdot 10^{-5}$  at 0.5 MeV incident neutron energy. Calculation of the detector efficiency and simulation of pulse height of the proton recoil counter is accomplished with a Monte-Carlo program. Detailed calculations and measurements have demonstrated that this system is capable of measuring neutron fluxes to an accuracy of 2 - 3 %. In particular, this detector has been used for the measurements described in section II.C.

The detector assembly at the right side of fig. 15 was developed by Cierjacks and Schouky for flux measurements in the energy region from a few MeV to 30 MeV. The assembly consists of three optically separated gas scintillation chambers filled with xenon at atmospheric pressure. High energy protons from the radiator foil at the entrance to the detector are identified by coincident events in all three chambers and by the specific energy loss of protons in the xenon gas. Energy losses in 10 cm of xenon of 30 and 6 MeV protons are approximately 0.5 and 2.5 MeV, respectively. Therefore, application of this telescope is restricted

to flux measurements for neutrons with energies higher than a few MeV. Since relative thick radiator foils can be used, the overall detector efficiency lies between  $1 - 4 \cdot 10^{-4}$  for neutron energies from 30 to 6 MeV. After some test runs which demonstrated the overall reliability of the telescope, the detector assembly was used in a recent measurement which aims for absolute determination of  $^{235}\text{U}$  and  $^{238}\text{U}$  fission cross sections. The calculation of the energy dependence of the absolute neutron flux from the cyclotron source is underway.

#### V. Planned Cross Section Measurements

Neutron cross section measurements in Karlsruhe will be pursued in 1972 and 1973 with unreduced man-power and budget. The following experiments are planned for this period:

At the Van-de-Graaff accelerator new measurements of the shape of  $\alpha$  versus energy for  $^{239}\text{Pu}$  and  $^{241}\text{Pu}$  are in preparation for an enlarged energy region from 10 - 400 keV. The 800 l scintillator tank will be employed for this application. New absolute fission cross section measurements are planned by Käppeler for  $^{239}\text{Pu}$  and  $^{241}\text{Pu}$  in the energy region from a few hundred keV to 1.2 MeV. Beer, Spencer and Ernst will measure additional high resolution capture data for the nuclei  $^{62}\text{Ni}$ ,  $^{64}\text{Ni}$ ,  $^{52}\text{Cr}$  and  $^{238}\text{U}$  between 10 - 200 keV. A precision measurement of the total cross section of  $^{10}\text{B}$  between 10 - 200 keV is in progress. Preparations are being made to determine the number of neutrons per fission  $\bar{\nu}$  of  $^{239}\text{Pu}$  from 50 - 1000 keV.

At the cyclotron the future activity will concentrate on measurements of differential elastic scattering cross sections of C, O, Na. High priority has been assigned to a measurement of the  $(n,n'\gamma)$ -cross section of  $^{238}\text{U}$ . An additional fission cross section measurement for  $^{240}\text{Pu}$  is in progress. It is planned to measure the fission cross section  $^{241}\text{Pu}$  in 1973. Work is in progress to improve the existing three-parameter facility used in experiments on  $(n,x)$ -reactions. With the improved facility  $(n,\alpha)$ -cross sections of Cr, Fe and Ni will be determined between a few and 30 MeV.

References

1. F.J.M. Farley, J. Nuclear Energy 3 (1956) 33
2. G. de Saussure et al., Nucl. Data for Reactors II, p. 223, IAEA Vienna (1967)
3. J.C. Hopkins, B.C. Diven, Nucl. Sci. Eng. 12 (1962) 169
4. H. Alter, C.L. Dunford, AI-AEC-MEMO-12916 (1970)
5. M.G. Schomberg et al., 2nd Intern. Conf. on Nucl. Data for Reactors I, 315, Helsinki (1970)
6. J.A. Farrell, G.F. Auchampaugh, M.S. Moore, P.A. Seeger, 2nd Intern. Conf. on Nucl. Data for Reactors I, 543, IAEA, Helsinki (1970)
7. J. Trochon, H. Derrien, B. Lukas, A. Michaudon, 2nd Intern. Conf. on Nucl. Data for Reactors I, 495, IAEA, Helsinki (1970)
8. K.N. Müller, G. Rohr, Nucl. Phys. A 164 (1971) 97
9. A.M. Lane, Ann. Phys. (N.Y.) 63 (1971) 171
10. R.G. Stieglitz, R.W. Hockenbury, R.C. Block, Nucl. Phys. A 163 (1971) 592
11. P.K. Butler, R.K. Sjoblom, Phys. Rev. 124 (1961) 1129
12. H.L. Smith, R.K. Smith, R.L. Henkel, Phys. Rev. 125 (1962) 1329
13. B.H. Patrick, M.G. Sowerby, M.G. Schomberg, EANDC (UK) 119 A1.
14. P.H. White, J. Nucl. Energy 19 (1965) 325
15. I. Szabo et al., Neutron Standards and Flux Normalization, AEC-Symposium, Series 23, p. 257 (1971)

16. G.N. Smirenkin et al. Atomnaya Energiya 13 (1963) 974
17. W.P. Pönitz, Neutron Standards and Flux Normalization, AEC-Symposium, Series 23, p. 281 (1971)
18. B. Block, H. Feshbach, Ann. Phys. 23 (1963) 471
19. J. Nebe, G.J. Kirouac, Kernforschungszentrum Karlsruhe Report, KFK-1189 (1970) and G.J. Kirouac, J. Nebe, Kernforschungszentrum Karlsruhe Report KFK-1069 (1969)
20. G.J. Kirouac, J. Nebe, Nucl. Phys. A 154 (1970) 36
21. J. Nebe, G.J. Kirouac, Nucl. Phys. A 185 (1972) 113
22. W. Hart, Report AHSP (S) R 169 (1969)
23. R.K. Smith, R.L. Henkel, R.A. Nobles, Bull. Am. Phys. Soc. 2, (1957) 196
24. P.H. White, G.P. Warner, EANDC (UK) 77 S (1969)
25. C.D. Bowman, E.G. Bilpuch, H.W. Newson, Ann. Phys. 17 (1962) 319
26. R.M. Wilenzick, G.E. Mitchell, K.K. Seth, H.M. Lewis, Phys. Rev. 121 (1961) 1150

TABLE 1 Resonance Parameter

$^{50}_{Cr} + n$

$E_{\lambda}$ (keV)	$g \Gamma_n$ (keV)	l
28.426 + .006	0.415 + .006	0
37.32 + .01	2.24 + .02	0
54.993 + .007	0.281 + .008	0
64.79 + .03	0.043 + .006	0
94.75 + .03	1.67 + .04	0
111.80 + .08	0.09 + .02	0
114.78 + .08	0.12 + .02	0
129.01 + .07	0.54 + .05	0
156.57 + .06	1.23 + .07	0
162.45 + .07	0.75 + .05	0
185.21 + .06	3.5 + .1	0
218.3 + .3	0.17 + .04	0
231.6 + .1	0.94 + .06	0
245.6 + .4	0.20 + .05	0
276.6 + .2	1.9 + .1	0
$\approx 289.8$	$\approx 3.7$	0

$a_0 = 4.2 + .1 \text{ fm}$   
 $S_0 = (3 + 1) \times 10^{-4}$

$^{64}_{Ni} + n$

$E_{\lambda}$ (keV)	$g \Gamma_n$ (keV)	l
14.3 + .2	2.9 + .5	0
33.81 + .04	8.90 + .05	0
106.52 + .08	0.11 + .03	0
129.32 + .03	1.34 + .04	0
141.97 + .09	0.17 + .02	0
148.8 + .2	0.08 + .02	0
154.96 + .04	3.89 + .07	0
163.2 + .1	0.14 + .02	0
177.70 + .05	0.47 + .03	0
191.5 + .1	0.16 + .03	0
205.3 + .2	0.06 + .02	0
214.7 + .3	0.08 + .02	0
219.8 + .1	0.03 + .02	0
226.9 + .3	0.12 + .03	0
231.95 + .04	3.77 + .09	0
237.9 + .1	0.32 + .04	0
255.7 + .3	0.17 + .04	0
269.68 + .07	2.21 + .09	0
283.5 + .4	0.35 + .07	0

$a_0 = 6.4 + .1 \text{ fm}$   
 $S_0 = (2 + 1) \times 10^{-4}$

TABLE 2 Neutron Resonance Parameters<sup>a)</sup> for n + <sup>40</sup>Ca

$E_\lambda$ (keV)	l	J	$\Gamma_n$ (keV)	$E_\lambda$ (keV)	l	J	$\Gamma_n$ (keV)
88.0 <sup>b)</sup>	0	1/2	0.15	993.0	(2)	(3/2)	1.1
132.0 <sup>b)</sup>	0	1/2	2.54	1004.0	0	1/2	11.0
144.0 <sup>b)</sup>	0	1/2	0.19	1019.0	1	(3/2)	0.5
167.0 <sup>b)</sup>	0	1/2	2.49	1025.0	(1)	(1/2)	0.3
220.0 <sup>b)</sup>	0	1/2	5.65	1037.0	1	1/2	0.7
250.0 <sup>b)</sup>	0	1/2	20.0	1041.0			
299.0 <sup>b)</sup>	0	1/2	2.19	1046.0			
338.0 <sup>c)</sup>	0	1/2	13.65	1056.0			
360.0 <sup>c)</sup>	0	1/2	1.50	1058.0	(1)	1/2	0.4
448.0 <sup>c)</sup>	0	1/2	13.38	1062.0	(1)	1/2	0.4
504.0 <sup>c)</sup>	0	1/2	10.65	1083.0	(1)	3/2	0.7
559.0	≠1			1094.0	2	(3/2)	0.6
570.0	1	3/2	0.2	1095.0	0	1/2	12.0
591.0	0	1/2	55.0	1098.0	2	5/2	0.2
594.0	2	5/2	< 0.1	1126.0	2	3/2	0.5
615.0	(2)	(3/2)		1129.0	2	3/2	0.7
624.0	2	5/2	< 0.1	1144.0	(1)	(3/2)	
636.0	0	1/2	2	1160.0	1	3/2	0.2
638.0	2	5/2	< 0.1	1169.0	1	3/2	0.7
641.0	1	1/2	1.3	1189.0	0	1/2	3.0
652.0				1203.0	1	3/2	4.0
668.0	2	(5/2)	< 0.1	1211.0	0	1/2	15.0
675.0	0	1/2	2.7	1214.0	1	3/2	1.0
695.0	1	1/2	0.9	1232.0	2	3/2	1.0
713.0	1	3/2	0.1	1243.0	1	1/2	1.5
728.0	1	3/2	< 0.1	1250.0	2	5/2	0.5
738.0	0	1/2	3.2	1262.0	(2)	(3/2)	0.5
743.0	0	1/2	4.4	1267.0	1	(3/2)	
747.0	1	1/2	0.3	1284.0	0	1/2	15.0
758.0	2	(3/2)	0.6	1289.0	2	(3/2)	
765.0	(1)	(3/2)	0.1	1308.0	(1)		
772.0	0	1/2	12.0	1318.0	(0)	(1/2)	
793.0	0	1/2	2.4	1333.0			
800.0	2	5/2	0.1	1337.0			
823.0	0	1/2	3.5	1348.0	1	3/2	
826.0	(1)	(1/2)	0.4	1355.0			
830.0	2	(5/2)	0.1	1375.0	0	1/2	
843.0	2	3/2	0.9	1388.0			
857.0	2	3/2	0.3	1408.0	1	1/2	
862.0	0	1/2	29.0	1424.0			
868.0	1	(1/2)	0.3	1433.0	0	1/2	11.0
879.0	0	1/2	31.0	1445.0	1	3/2	
885.0	1	3/2	0.3	1452.0	1	3/2	
908.0	1	1/2	1.5	1468.0			
925.0	2	5/2	0.2	1478.0	1		
941.0	1	1/2	0.6	1489.0	(1)		
945.0	2	3/2	0.5	1494.0			
959.0	1	3/2	0.4	1515.0			
970.0	0	1/2	7.2	1530.0	2	5/2	
983.0							

a) The analysis has been performed with a channel radius of 3.59 fm and a boundary condition  $S_1 = B_1(E)$ . The accuracy of level widths greater than 0.5 keV is estimated to be better than 20%. b) Data from ref. 25. c) Data from ref. 26.

Figure Captions:

- Fig. 1 Experimental setup for the measurement of capture-to-fission ratios.
- Fig. 2 Ratio of capture-to-fission for  $^{239}\text{Pu}$ .
- Fig. 3 Ratio of capture-to-fission for  $^{235}\text{U}$ .
- Fig. 4 Transmission of  $^{50}\text{Cr}$ -oxide for two different sample thicknesses; the solid curve represents a multilevel least squares fit.
- Fig. 5  $^{57}\text{Fe}$  capture yield divided by sample thickness versus energy.
- Fig. 6 Typical fission detectors used in ratio and absolute measurements.
- Fig. 7 Fission cross section ratio  $^{241}\text{P}/^{235}\text{U}$ .
- Fig. 8 Absolute fission cross section of  $^{235}\text{U}$  (preliminary).
- Fig. 9 Experimental setup for the measurement of  $\gamma$ -ray production cross section.
- Fig. 10 Cross section for the production of the 2209 keV  $\gamma$ -ray from inelastic scattering in iron.
- Fig. 11 Differential neutron scattering cross section for  $^{40}\text{Ca}$  from 0.75 - 1.15 MeV.
- Fig. 12 Schematic view of the scattering chamber used for (n,x)-reaction cross section measurements.
- Fig. 13 Differential excitation functions for the  $^9\text{Be}(n,\alpha)$ -reaction for six characteristic angles between  $20^\circ$  and  $140^\circ$ .
- Fig. 14 Fission cross section ratio  $^{238}\text{U}/^{235}\text{U}$  (preliminary).
- Fig. 15 Schematic drawing of proton telescopes used for absolute neutron flux determination.





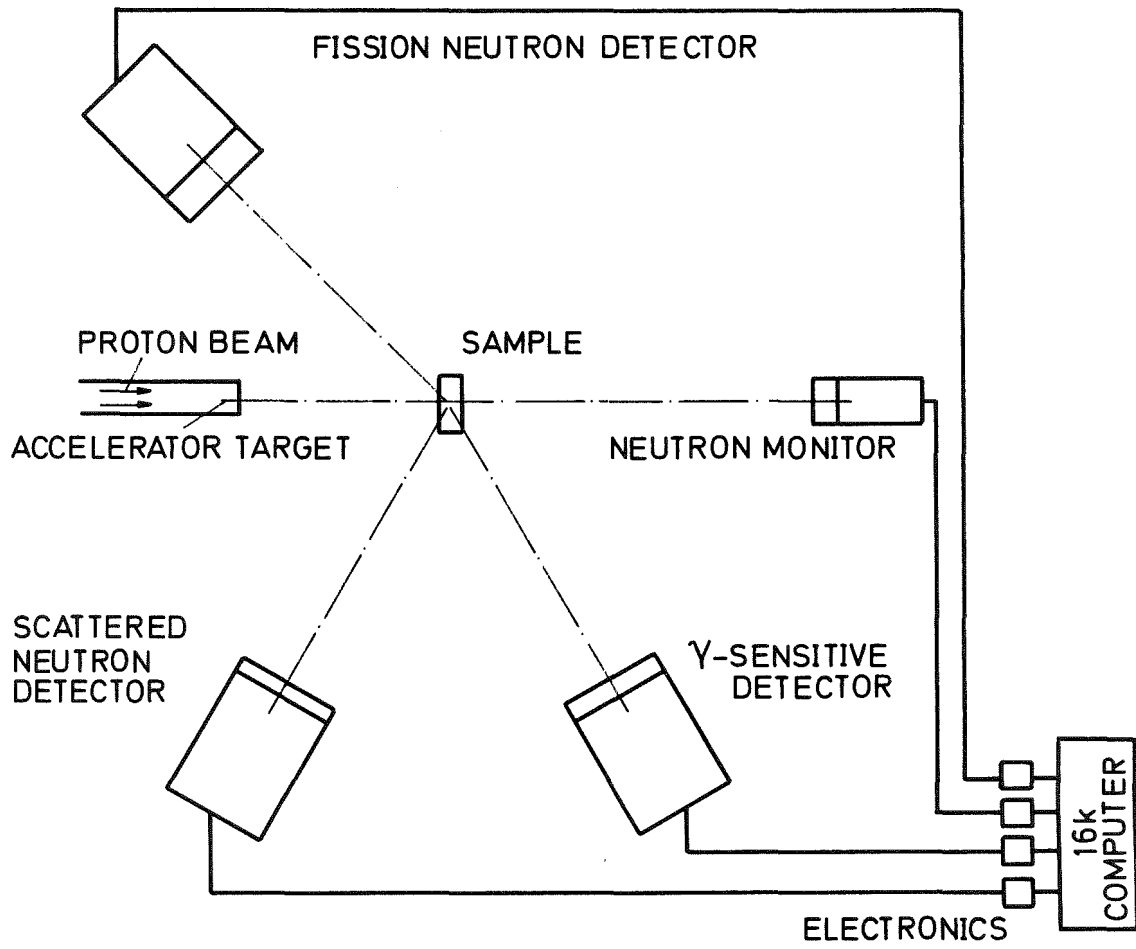


Fig. 1

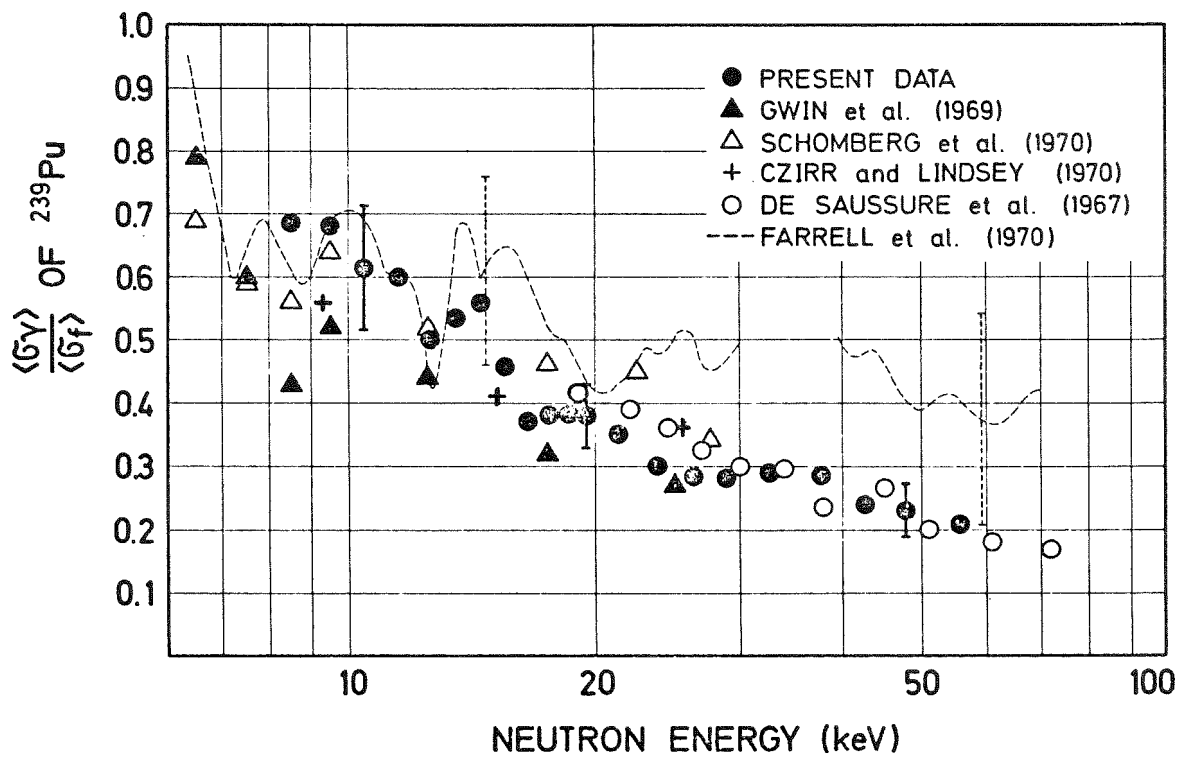


Fig. 2

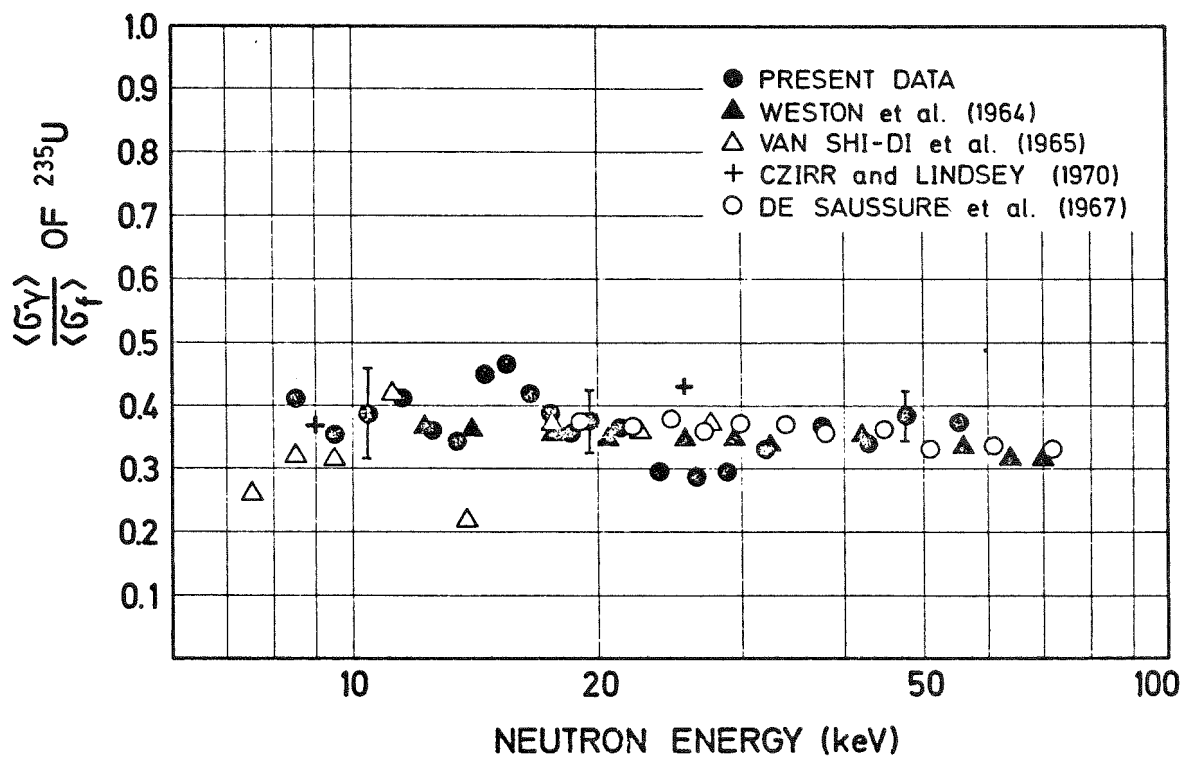


Fig. 3

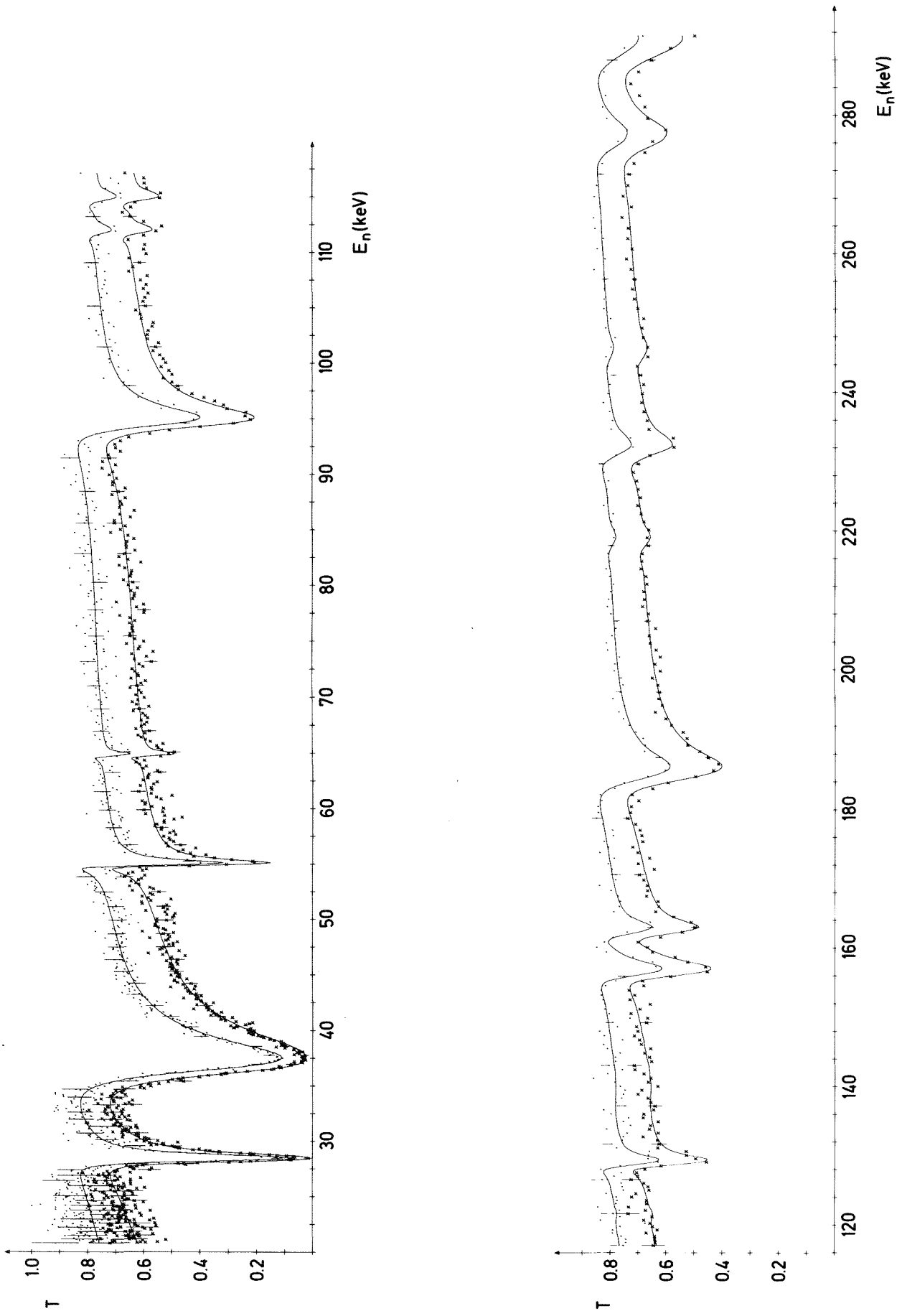


Fig. 4

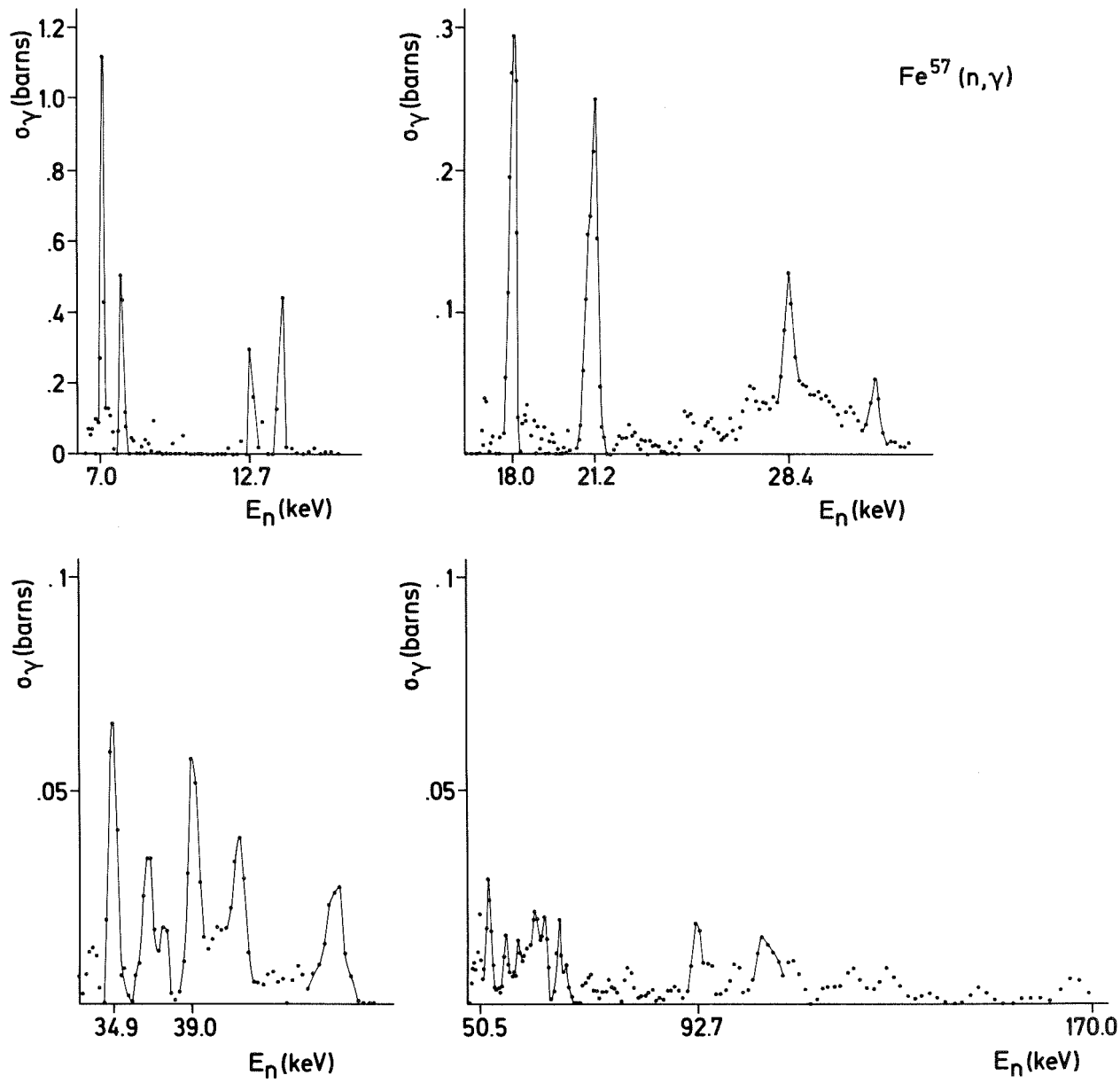


Fig. 5

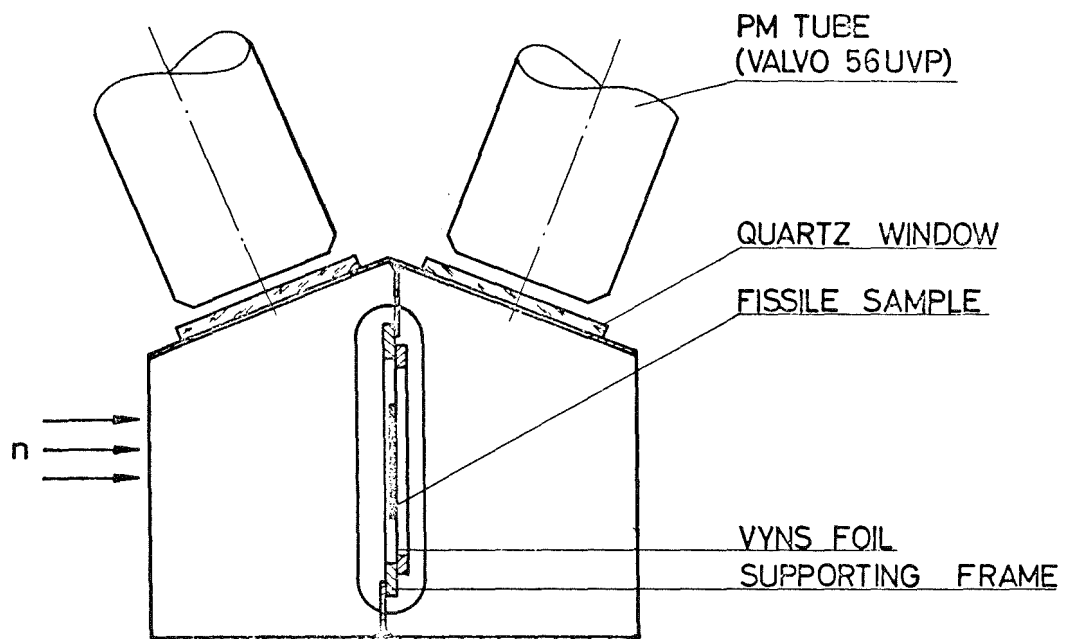
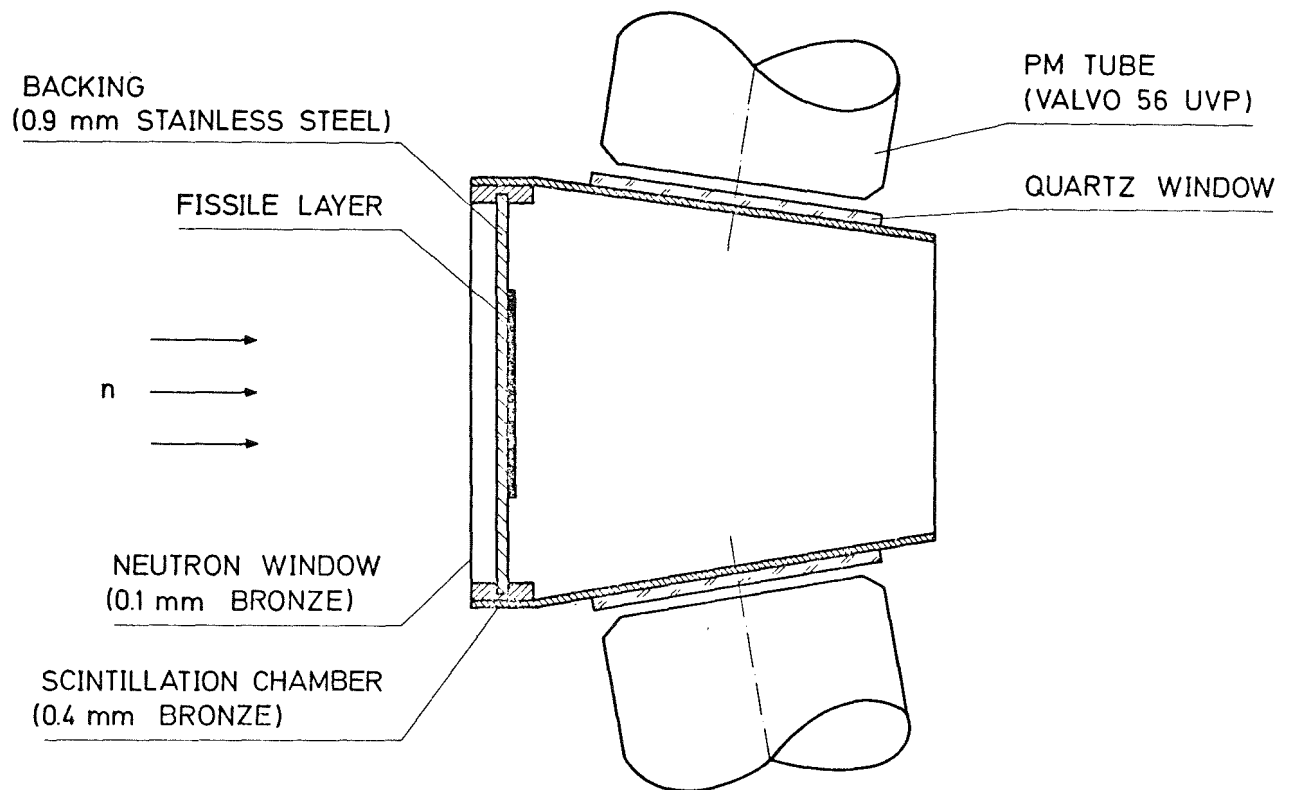


Fig. 6

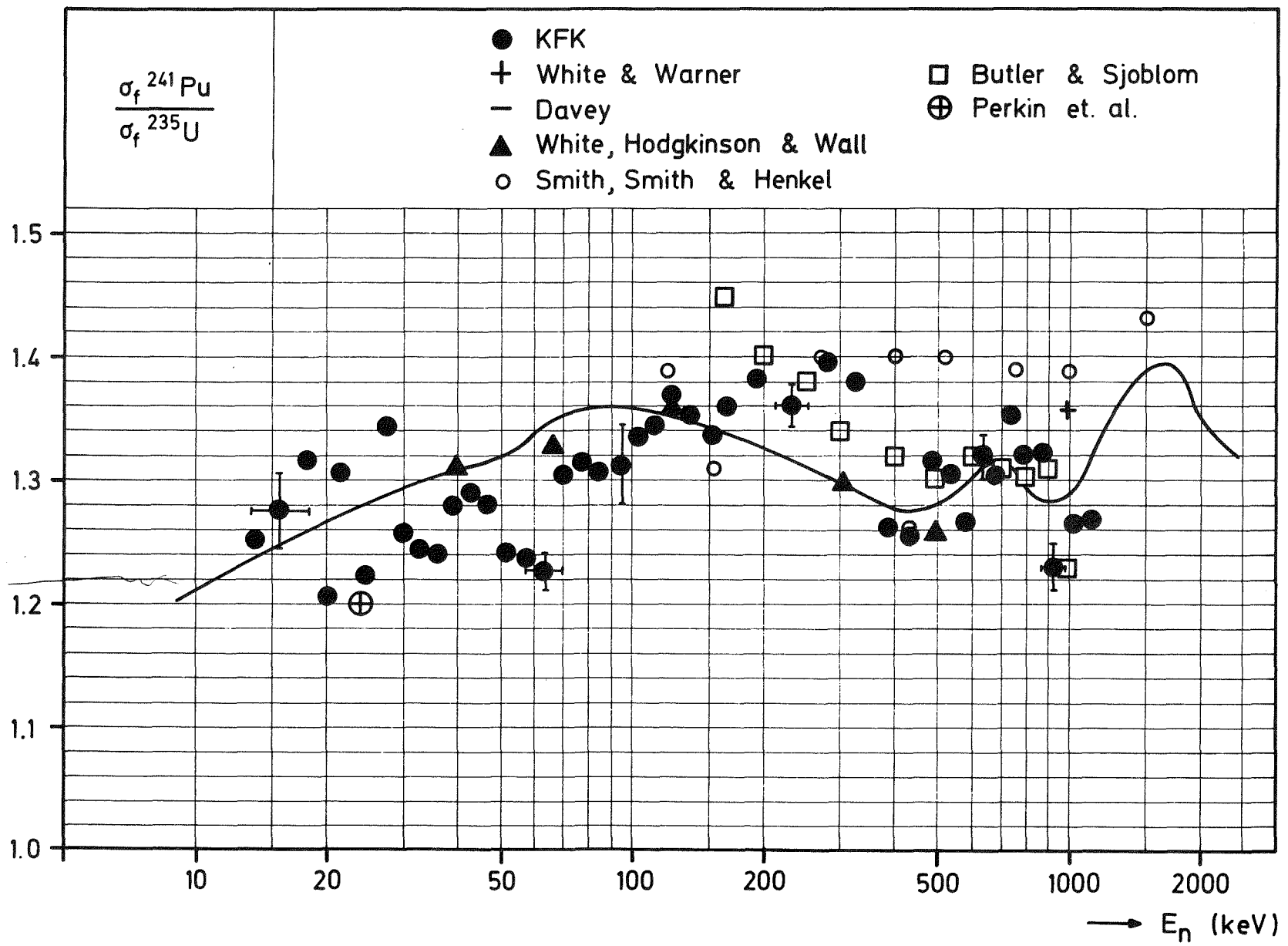


Fig. 7

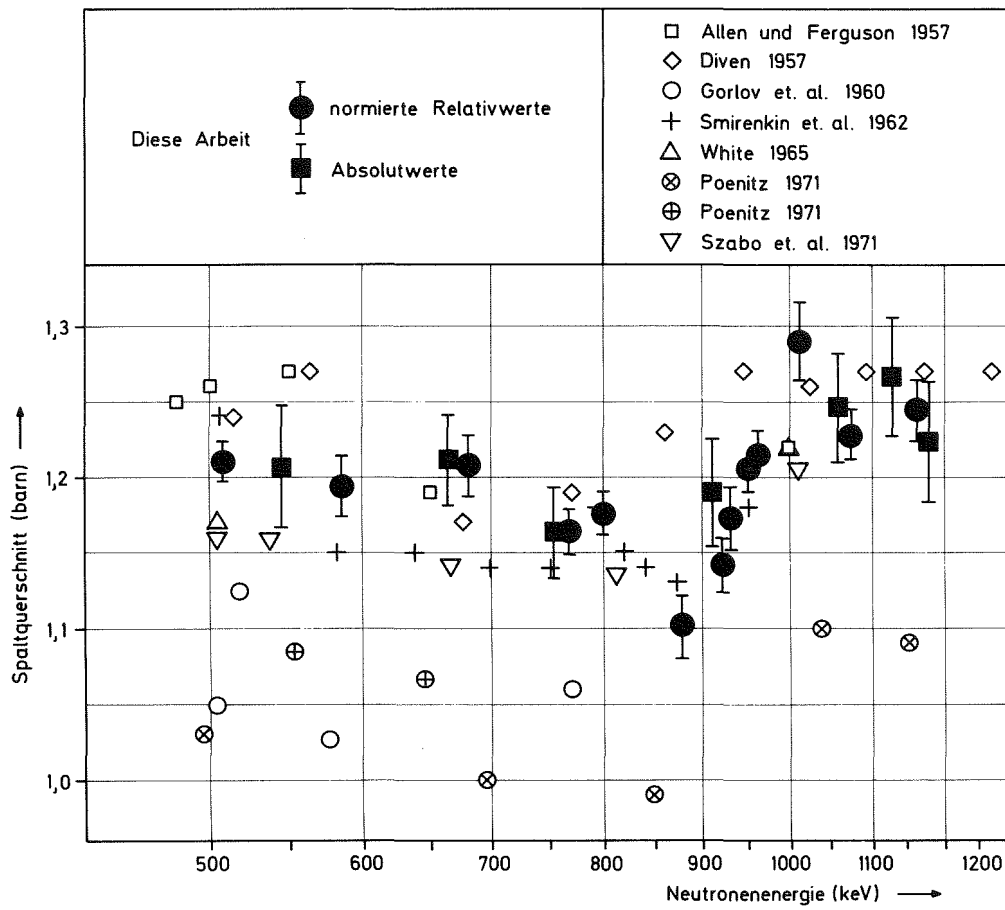


Fig. 8

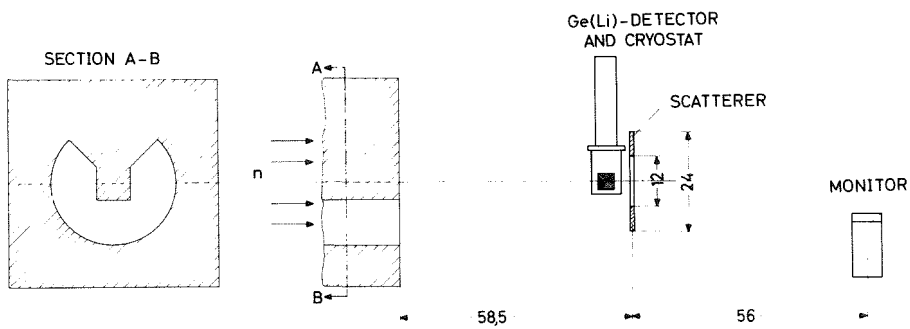


Fig. 9

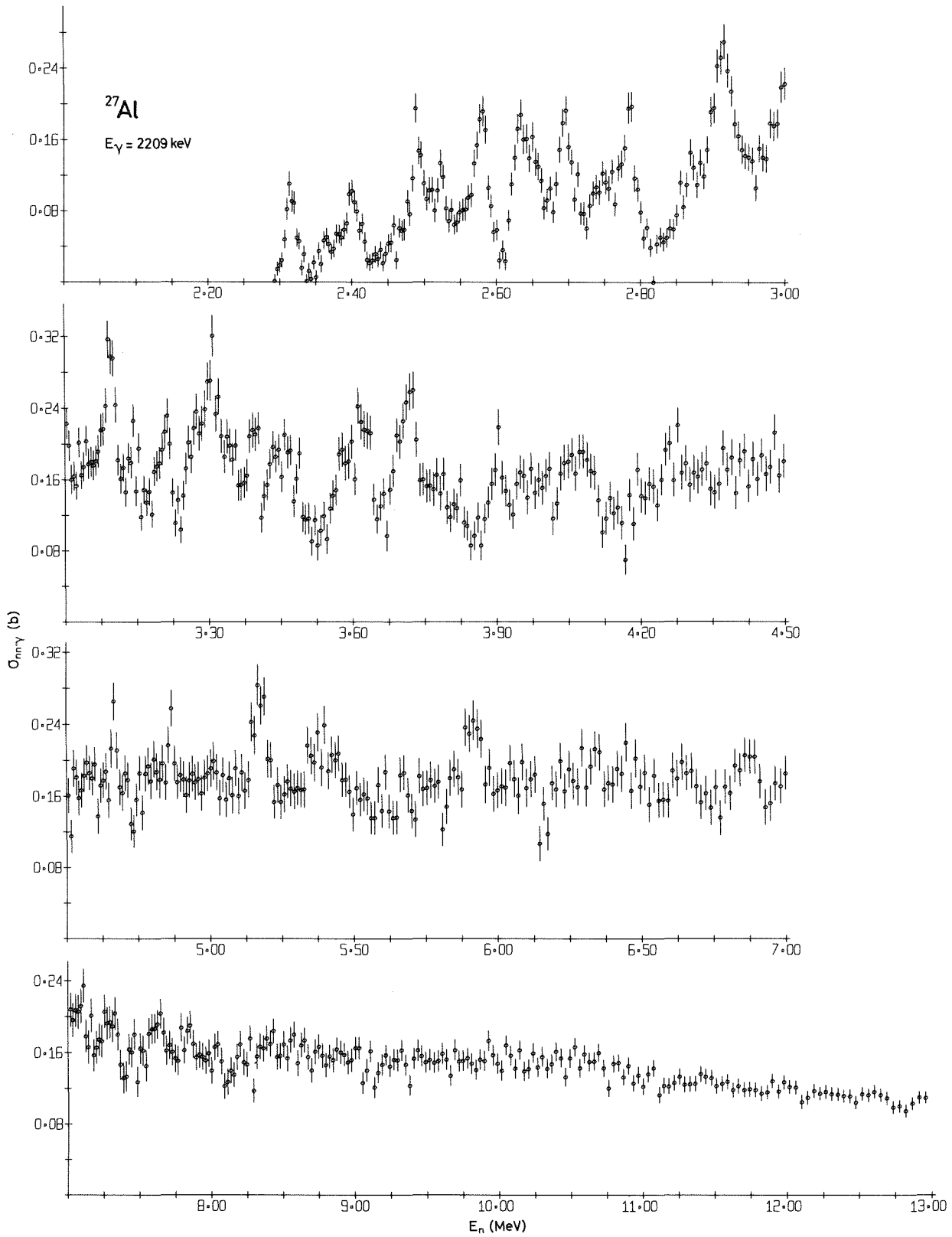


Fig. 10



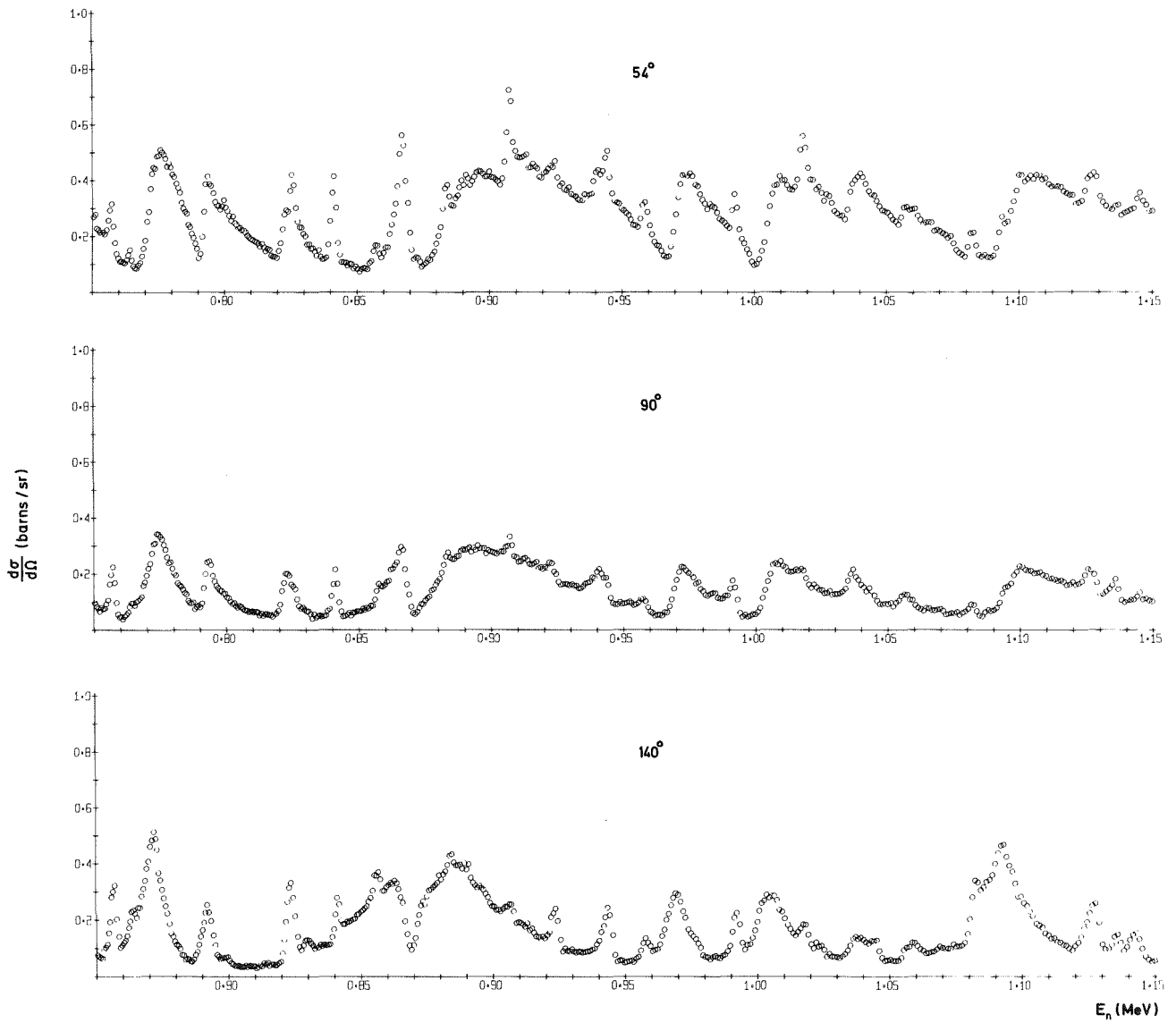


Fig. 11

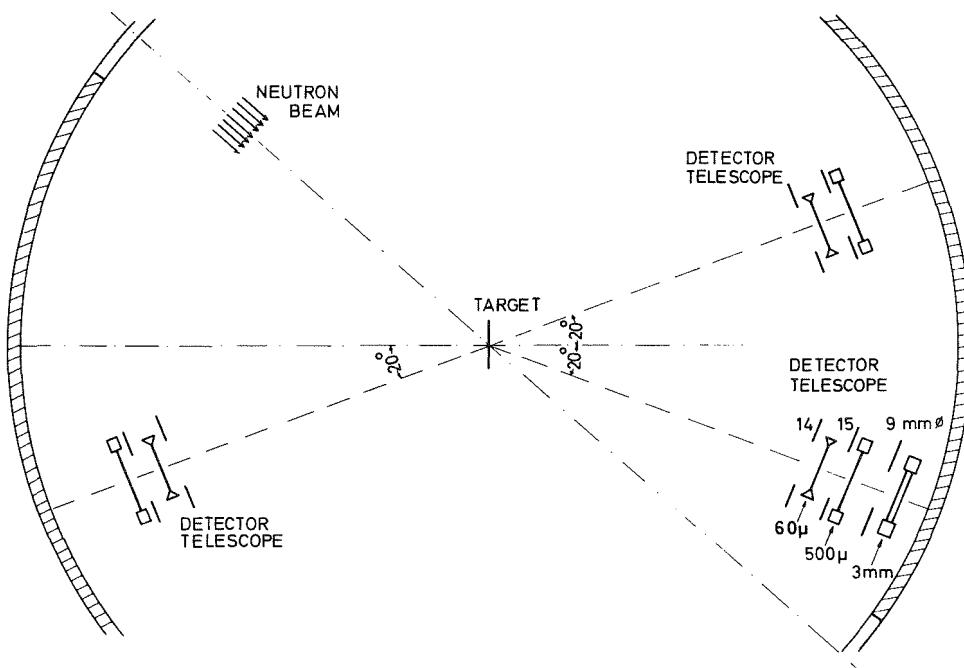


Fig. 12

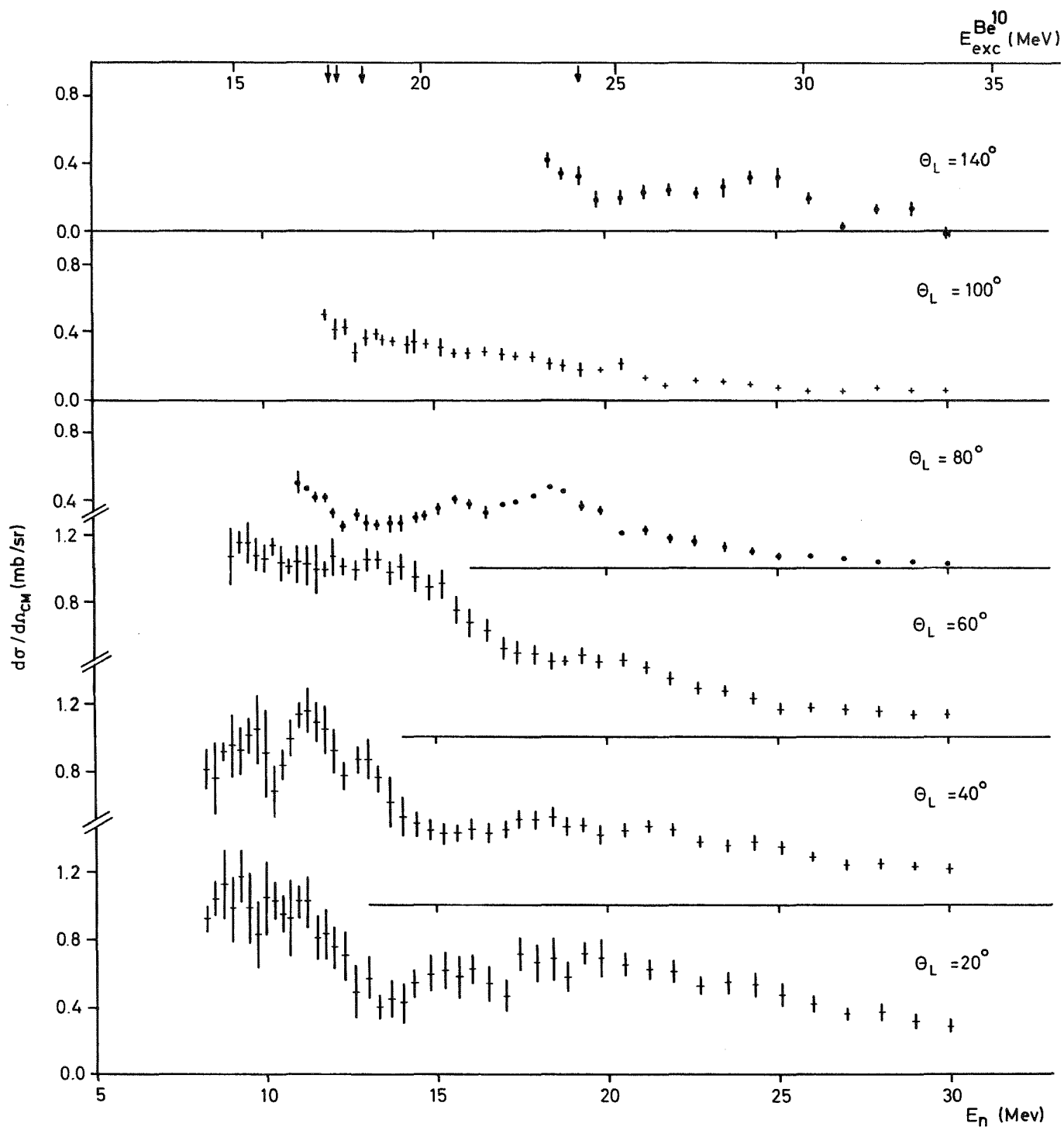


Fig. 13

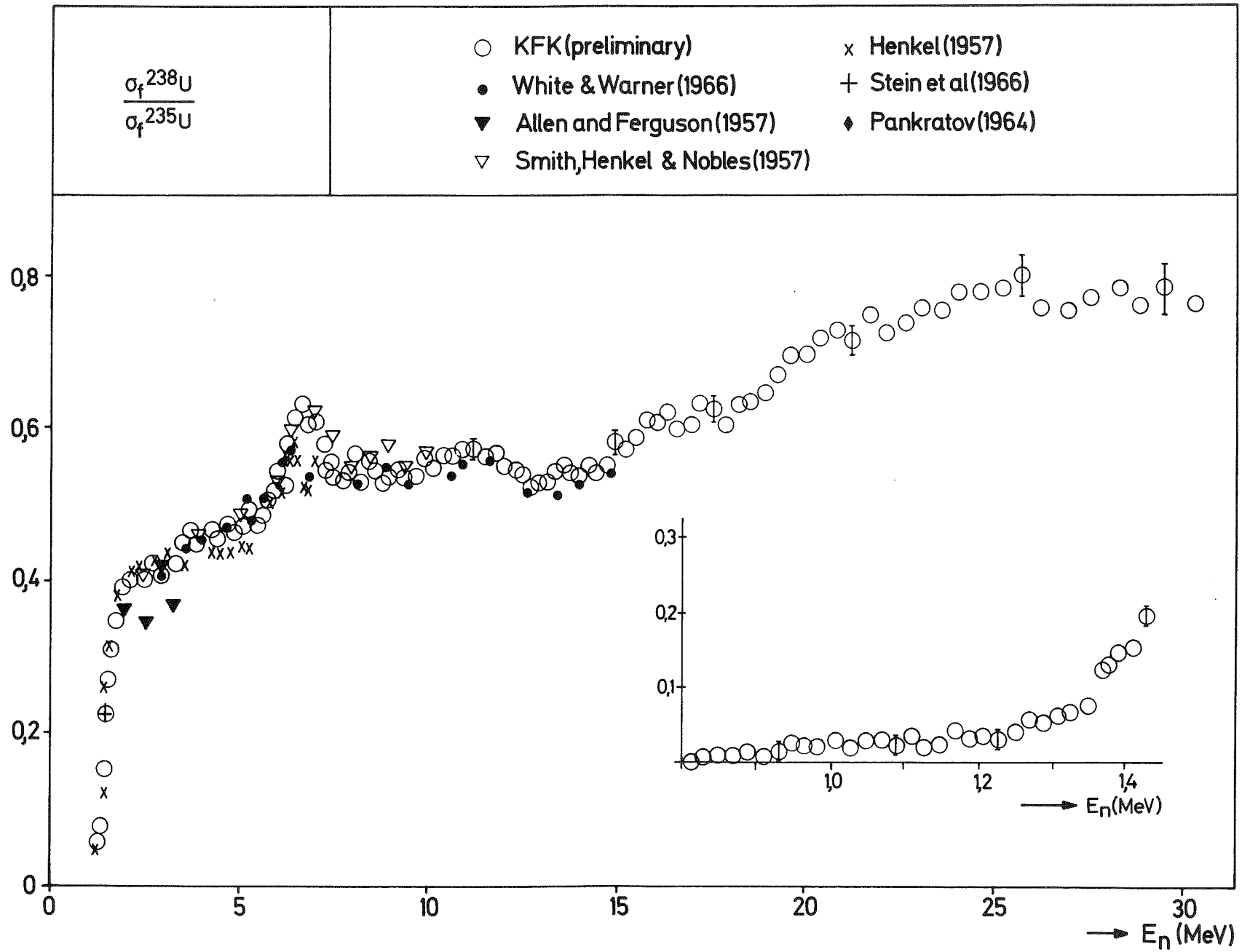


Fig. 14

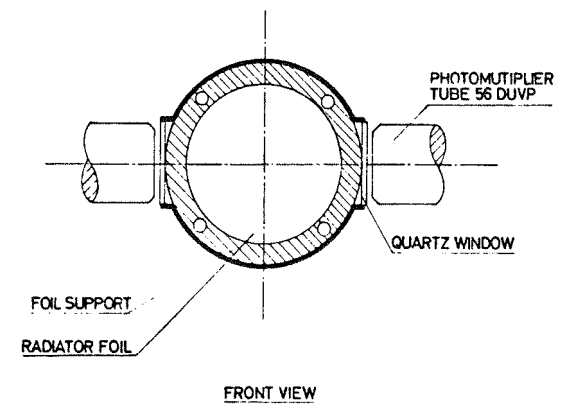
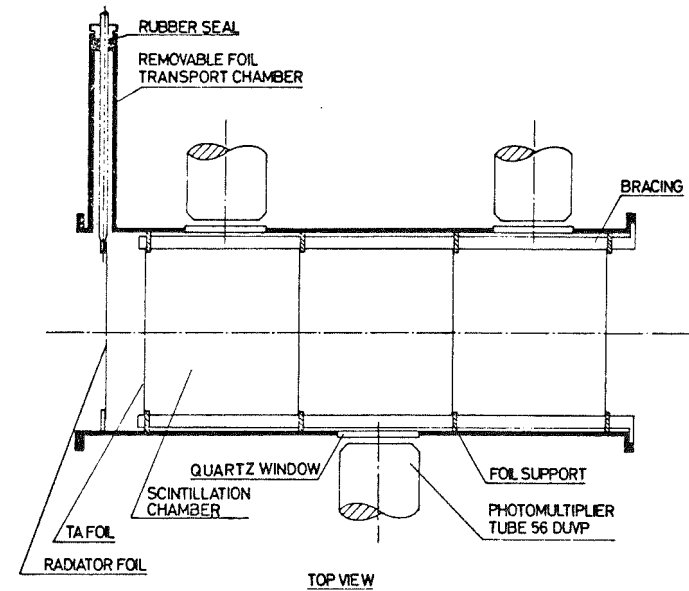
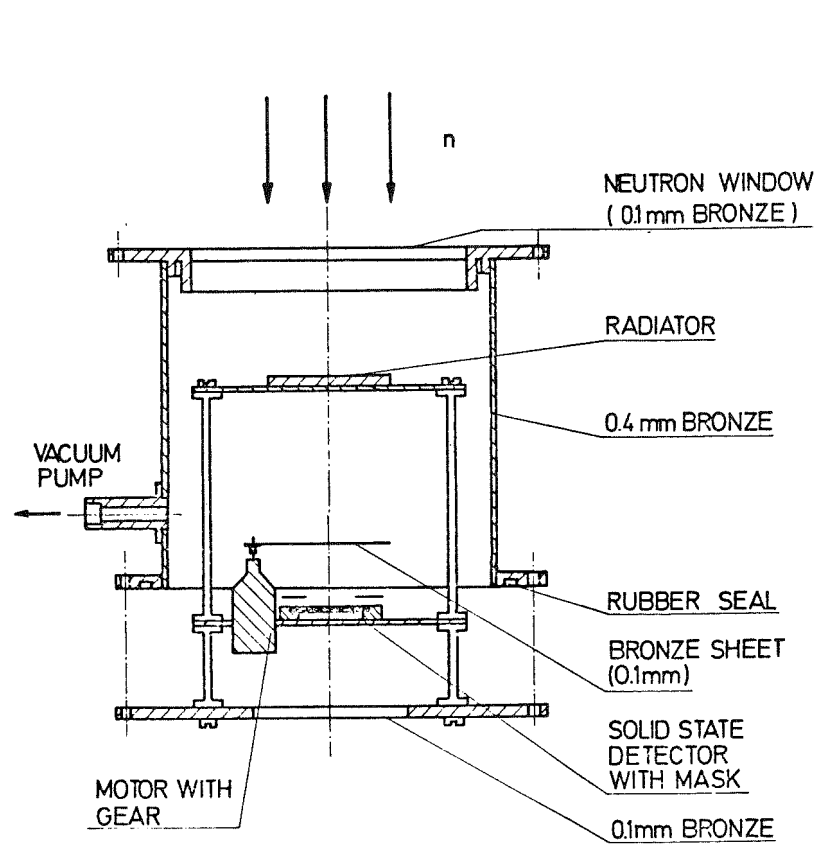


Fig. 15